Detailed Kinematic Study of the Ionized and Neutral Gas in the Complex of Star Formation in the Galaxy IC 1613*

T.A. Lozinskaya[1], A.V. Moiseev[2], and N.Yu. Podorvanyuk[1]

[1] Sternberg Astronomical Institute, Universitetskii pr. 13, Moscow, 119899 Russia
[2] Special Astrophysical Observatory, Nizhniĭ Arkhyz, Karachai–Cherkessia, Russia, 369167 Russia

Received August 20, 2002

Abstract. We carried out detailed kinematic studies of the complex of multiple H I and H II shells that represent the only region of ongoing star formation in the dwarf irregular galaxy IC 1613. We investigated the ionized-gas kinematics by using Fabry–Perot Hα observations with the 6-m Special Astrophysical Observatory telescope and the neutral-gas kinematics by using VLA 21-cm radio observations. We identified three extended (300–350 pc) neutral shells with which the brightest H II shells in the complex of star formation are associated. The neutral-gas kinematics in the complex has been studied for the first time and the H I shells were found to expand at a velocity of 15–18 km s^{-1}. We constructed velocity ellipses for all H II shells in the complex and refined (increased) the expansion velocities of most of them. The nature of the interacting ionized and neutral shells is discussed.

1. INTRODUCTION

The giant complex of multiple ionized shells (Meaburn *et al.* 1988) in the northeastern sector of I 1613 is the most prominent structure in narrow-band images of this Local-Group dwarf irregular galaxy located at a distance of 725–730 kpc (Freedman 1988a, 1988b; Dolphin *et al.* 2001) in the Hα, [O III], and [S II] lines.

Most of the bright H II regions (Sandage 1971; Lequeux *et al.* 1987; Hodge *et al.* 1990; Price *et al.* 1990; Hunter *et al.* 1993; Valdez-Gutierrez *et al.* 2001) and the only known supernova remnant in the galaxy [Lozinskaya *et al.* (1998) and references therein] belong to this complex.

The stellar population of the complex is represented by some twenty young stellar associations and clusters (Hodge 1978; Georgiev *et al.* 1999; and references therein).

This multishell complex and the rich stellar grouping represent the only site of ongoing star formation in the galaxy. This region of violent star formation in IC 1613 can probably be considered as a very young and small superassociation (Lozinskaya 2002a).

Recent 21-cm radio observations of the complex have shown that extended neutral shells (supershells in standard terminology) are associated with multiple ionised shells (Lozinskaya et al 2001, 2002; Lozinskaya 2002b).

The ionized-gas velocities in the region were first measured by Meaburn *et al.* (1988); five spectrograms for the bright part of the complex with poor spatial coverage were used to determine the characteristic expansion velocities of the H II shells, ~ 30 km s^{-1}. Valdez-Gutierrez *et al.* (2001) constructed the ionized-gas radial-velocity field in the Hα and [S II] lines all over the galaxy and estimated the shell expansion velocities from the splitting of the line profile integrated over each of the objects.

The H I and H II shells close up and partially overlap in the plane of the sky. If their sizes along the line of sight and in the plane of the sky are assumed to be comparable, then they can be assumed to be in physical contact with one another[1].

Deep narrow-band Hα images revealed a chain of bright compact emission-line objects at the boundary of the two closing shells in the complex. Spectroscopic observations show that the compact objects are early-type giants and supergiants (Lozinskaya *et al.* 2002). The characteristic ionized- and neutral-gas morphology suggests that the H I and H II shells physically interact in the region of the stellar chain (see also Section 3).

Thus, the complex of star formation shows evidence of the possible collision between expanding ionized and neu-

Send offprint requests to: T.A. Lozinskaya, e-mail: lozinsk@sai.msu.ru

* Based on observations collected with the 6m and 1m telescopes of the Special Astrophysical Observatory (SAO) of the Russian Academy of Sciences (RAS), operated under the financial support of the Science Department of Russia (registration number 01-43)

[1] The galaxy is inclined at an angle of 30° to the plane of the sky and the gaseous-disk thickness 500–700 pc, as estimated by Afanasiev *et al.* (2000), is comparable to the size of the multishell complex. Therefore, a chance projection of physically unrelated shells located at different distances is unlikely.

Date of observation	IFP type	T_{exp}, Å	Seeing
Nov. 1, 2000	IFP235	32×240	$2\farcs0$
Sep. 12, 2001	IFP501	36×200	$1\farcs8$

tral shells, the interaction of ionized shells with the surrounding H I shells, and the like. This evidence suggests that the birth of new-generation stars triggered by shell collisions is probable here (Chernin and Lozinskaya 2002). That is why a detailed study of the structure and kinematics of the ionized and neutral gas in the multishell complex is of current interest.

The neutral-gas kinematics in the complex of star formation has not yet been investigated.

Our goal is to study in detail the kinematics of the neutral and ionized gas components in the shells that constitute the complex of star formation with high spatial and spectral resolutions.

To study the kinematics of the ionized shells, we carried out Hα observations with a scanning Fabry–Perot interferometer attached to the 6-m Special Astrophysical Observatory (SAO) telescope. The kinematics of the neutral shells was studied by using VLA 21-cm radio observations.

The techniques for optical and radio observations and for data reduction are described in Section 2. In Section 3, we use the ionized- and neutral-gas observations to analyze the overall structure of the multishell complex in the plane of the sky. The results of our kinematic study for the H I and H II shells in the complex are presented in Sections 4 and 5, respectively. Our results and conclusions regarding the nature of the multishell complex that follow from them are discussed in Section 6.

2. INTERFEROMETRIC Hα AND 21 CM OBSERVATIONS

Fabry–Perot Observations with the 6-m SAO Telescope and Data Reduction

Interferometric Hα observations were carried out at the prime focus of the 6-m SAO telescope using a scanning Fabry–Perot interferometer (IFP). The interferometer was placed inside the SCORPIO focal reducer, so the equivalent focal ratio was ($F/2.9$). A brief description of the focal reducer is given in the Internet (http://www.sao.ru/ moisav/scorpio/scorpio.html); the SCORIO capabilities in IFP observations were also described by Moiseev (2002). The detector was a TK1024 1024×1024-pixel CCD array. The observations were performed with 2×2-pixel hardware averaging to reduce the readout time, so 512×512-pixel images were obtained in each spectral channel. The field of view was $4\farcm8$ for a scale of $0\farcs56$ per pixel. An interference filter with $FWHM = 15$ Å centered on the Hα line was used for premonochromatization.

We used two different Queensgate ET-50 interferometers operating in the 235th and 501st orders of interference at the Hα wavelength (designated in Table 1 as IFP235 and IFP501, respectively). IFP235 provided a spectral resolution of $FWHM \approx 2.5$ Å near the Hα line (or ~ 110 km s^{-1}). The separation between neighboring orders of interference, $\Delta\lambda = 28$ Å, corresponded to a range of ~ 1270 km s^{-1} free from order overlapping. The spectral resolution of IFP501 was ~ 0.8 Å (or ~ 40 km s^{-1}) for a range of $\Delta\lambda = 13$ Å (or ~ 590 km s^{-1}) free from order overlapping.

During the exposure, we sequentially took interferograms of the object for various IFP plate spacings. Therefore, the number of spectral channels was 32 and 36 and the size of a single channel was $\delta\lambda \approx 0.87$ Å (~ 40 km s^{-1}) and $\delta\lambda \approx 0.36$ Å (~ 16 km s^{-1}) for IFP235 and IFP501, respectively.

We reduced our interferometric observations by using the software developed at the SAO (Moiseev 2002). After the primary data reduction, the subtraction of night-sky lines, and wavelength calibration, the observational material represents "data cubes" in which each point in the 512×512-pixel field contains a 32-channel or 36-channel spectrum. We performed optimal data filtering — Gaussian smoothing over the spectral coordinate with $FWHM = 1.5$ channels and spatial smoothing by a two-dimensional Gaussian with $FWHM = 2 - 3$ pixels — by using the ADHOC software package[2].

The accuracy of the wavelength calibration using the calibration-lamp line was less than 3 km s^{-1}. Our radial-velocity measurements of the night-sky λ6553.617 Åline revealed a systematic shift when measuring the absolute values of the radial velocities: -8 ± 3 km s^{-1} for IFP501 and 15 ± 8 km s^{-1} for IFP235. It should be noted, however, that these values were most likely overestimated, because the sky-line intensity varied during the scanning time.

The bulk of the observational data used here were obtained with IFP501, which provided a higher spectral resolution. Only when analyzing the observational data for the supernova remnant, where the weak line wings were observed at velocities outside the range free from order overlapping for IFP501, did we additionally use observations with IFP235.

Observations in the 21 cm Line and Data Analysis

Based on VLA 21-cm observations, we mapped the H I distribution with a high angular resolution and studied the neutral-gas kinematics in an extended region of the galaxy that included the complex of star formation. An application for the project to study the neutral-gas struc-

[2] The ADHOC software package was developed by J. Boulestex (Marseilles Observatory) and is publicly available in the Internet.

the first results were published by Lozinskaya *et al.* (2001).

The data given in Sections 3 and 4 were obtained by combining VLA observations in configurations B, C, and D; the width of a single channel in radial velocity was 2.57 km s^{-1}. We smoothed the data with the Hunning function. The data were calibrated by the standard method and transformed into maps using the AIPS software package.

The reduced data are presented in the form of a data cube with an angular resolution of $7''.4 \times 7''.0$, which corresponds to a linear resolution of ~ 23 pc.

To map the integrated 21-cm line intensity distribution, we summed only 40 of the 127 possible spectral channels, because no galactic line emission was detected in the remaining channels.

3. THE OVERALL STRUCTURE OF THE COMPLEX OF STAR FORMATION IN THE PLANE OF THE SKY

Figure 1 shows the monochromatic Hα image of the multishell complex obtained by integrating the emission over all spectral channels (in the velocity range from -2 to -584 km s^{-1}) using our interferometric observations with IFP501. The arrows indicate the objects discussed in Section 5: the chain of early-type giants and supergiants mentioned above, the only Of star in the galaxy identified by Lozinskaya *et al.* (2002), the only known supernova remnant — the nebula S8 (Sandage 1971), and the bright H II region no. 40a, b from the list by Hodge *et al.* (1990). Also shown in the figure are the ionized-shell numbers from the list by Valdez-Gutierrez *et al.* (2001). (Below, we use the notation adopted in this paper for uniformity.)

All of the brightest ionized shells in IC 1613 are concentrated in the complex of star formation (Valdez-Gutierrez *et al.* 2001; Lozinskaya *et al.* 2002). In Fig. 1a, these brightest regions are overexposed to show the faintest H II shells. The faint filamentary structures in shells R6, R7, R8, and R3 are clearly seen in the figure; we also managed to detect weak emission from thin filaments in several other regions of the complex.

The chain of bright early-type stars is located at the bright boundary of the ionized shell R1 adjacent to shell R2. This region falls within square N27 in Fig. 3 from Valdez-Gutierrez *et al.* (2001) and includes the nebulae S10 and S13, according to the classification of Sandage (1971). Association no. 17 from the list by Hodge (1978) [its eastern part is designated as no. 25 in the list by Georgiev *et al.* (1999)] also lies here.

Our 21-cm H I observations in IC 1613 with a high angular resolution allow us to compare the H I and H II distributions in the complex of star formation. The results obtained from these observations are presented in Figs. 1b and 2a. Figure 1b shows the 21-cm image of the northwestern galactic sector obtained by integrating the emission over 40 channels in the velocity range

imposed on the monochromatic Hα image (indicated by isophotes). The latter is represented only by the brightest regions. The H I intensity distribution in the entire galaxy is shown in Fig. 2a (see Section 4).

Even the first observations by Lake and Skillman (1989) with an angular resolution of $60'' \times 60''$ showed that the complex of ionized shells is localized in the region of the brightest spot on the H I map of IC 1613. The multishell structure of this bright spot is clearly seen in Figs. 1b and 2a: the three most prominent H I shells in the galaxy surround the chain of bright ionized shells. Below, these bright neutral shells are called I, II, and III for definiteness.

The central coordinates, sizes, and expansion velocities of the shells estimated in Section 4 are listed in Table 2. The third column gives the shell sizes along two axes in arcsec (upper row) and the mean radius in pc determined by them (lower row).

The shells identified in the star-forming region are 300–350 pc in size. These sizes fall within the region of the peak in the size distribution of giant H I and H II shells in the LMC and SMC (see Meaburn 1980; Kim *et al.* (1999); Staveley-Smith *et al.* (1997).

In addition to these three brightest and most prominent H I shells, we identified much larger ring-shaped and arc-shaped structures in IC 1613, with sizes up to 1–1.5 kpc, supergiant shells in the terminology of Meaburn (1980). These are clearly seen in the 21-cm image of the entire galaxy shown in Fig. 2a (see also Section 6).

As follows from Figs. 1a and 1b, a one-to-one correspondence between the neutral and ionized structures in size and localization is observed only in one case: the ionized shell R4 fits well into its surrounding neutral shell II. The remaining bright H II shells are smaller than the neutral shells and are located irregularly: the ionized shell R1 lies within the neutral shell I near its western boundary rather than in the central cavity; R6 lies within shell III near its eastern boundary; the ionized shells R2 and R5 fall on the bars between shells I and II and between shells II and III, respectively. As was shown by Kim *et al.* (1999), the giant H I shells in the LMC are also interrelated differently with H II shells and supershells, which reflects the different evolutionary stages of star formation in the region. This issue is discussed in more detail in Section 6.

The boundary of the ionized shell R1 with the chain of blue giants and supergiants coincides with the thinnest arc-shaped H I bar between the two H I shell structures. The characteristic morphology of the ionized and neutral shells suggests that they are in physical contact: the thin neutral arc adjoins the ionized shell in the region of the stellar chain from the outside and the two shells in this region have the same radius of curvature.

The stellar component of the complex represented by some twenty stellar associations and clusters is superimposed on the Hα and 21 cm images in Fig. 1c. The figure shows the association boundaries that correspond to a new breakdown of the stellar population into separate

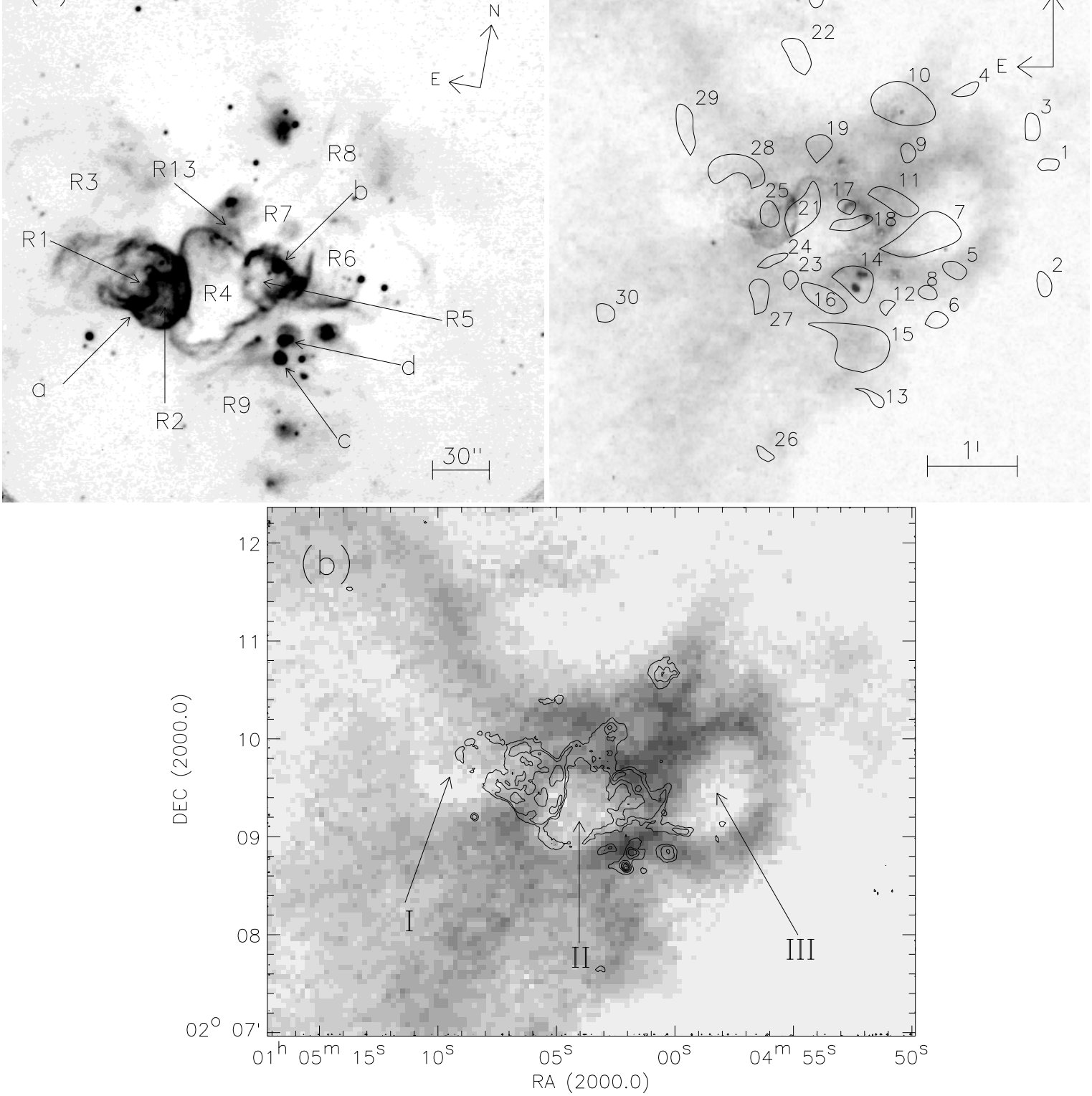

Fig. 1. (a) The monochromatic Hα image of the multishell complex obtained with a Fabry–Perot interferometer on the 6-m SAO telescope. The ionized shells R1–R9 and R13 from the list of Valdez-Guterrez *et al.* (2001) studied here are labeled. The arrows indicate: a "— the chain of early-type supergiants at the boundary of shell R1; b "— the only Of-type star identified by Lozinskaya *et al.* (2002); c "— the only supernova remnant in IC 1613; d "— object no. 40a, b from the list of H II regions by Hodge *et al.* (1990). (b) The H I intensity distribution (indicated by shades of gray) superimposed on the monochromatic Hα image of the region (the isophotes corresponding to the brightest regions in Fig. 1a are shown). The Roman numericals I, II, and III mark the three neutral shells investigated here. (c - *top right*) The boundaries of the OB associations identified by Georgiev *et al.* (1999) superimposed on the intensity distributions in the 21-cm line (indicated by shades of light gray) and in the Hα line (indicated by shades of dark gray) .

Shell	central coordinates (2000)	Size, arcsec R, pc	V(exp), km s^{-1}	Age, Myr
I	$1^{\rm h}5^{\rm m}10^{\rm s}$ $2^\circ9'45''$	~ 97 172		
II	$1^{\rm h}5^{\rm m}4.5^{\rm s}$ $2^\circ9'19''$	73×81 136	12–17	5.6
III	$1^{\rm h}4^{\rm m}58^{\rm s}$ $2^\circ9'32''$	73×97 150	16–18	5.3

groups in Georgiev *et al.* (1999). Here, a number of associations from the list by Hodge (1978) were split into several smaller groups.

4. NEUTRAL-GAS KINEMATICS IN THE COMPLEX

The data cube that we constructed from the 21-cm observations allows us to analyze the H I distribution and kinematics in the entire galaxy. The kinematics of the southeastern region of IC 1613 around a WO star was studied previously (Lozinskaya *et al.* 2001). Here, we consider in detail the neutral-gas kinematics in the complex of star formation for the first time.

Our 21-cm observations show that this complex stands out as the dynamically most active region in IC 1613. Velocities of internal neutral-gas motions from $-195 \div -200$ to $-250 \div -255$ km s^{-1} are observed in the region of the complex ($\Delta RA = 1^{\rm h}4^{\rm m}50^{\rm s} - 1^{\rm h}5^{\rm m}15^{\rm s}, \Delta D = 2^\circ07' - 2^\circ11'$) against the background of a smooth systematic variation in the mean H I velocity along the galaxy that was pointed out by Lake and Skillman (1989).

In searching for the possible expansion of the H I shells in the complex, we constructed position–radial velocity diagrams in several bands:

1 — in the band that crosses the pair of shells I and II through their centers;

2 — in the band that crosses the pair of shells II and III in the same way;

3 — in the band that passes through the stellar chain at the boundary of shells I and II;

4, 5, and 6 — in the bands that cross each of the three shells I, II, and III, respectively, in the directions perpendicular to scans 1 and 2;

7 — in the band that includes scans 15 and 16 in the Hα line (see Section 5) and that passes through the only supernova remnant in IC 1613.

The directions of scans 1–7 on the H I map are shown in Fig. 2a. The position–radial velocity diagrams constructed for these scans are shown in Fig. 2b.

We chose the band width when scanning in such a way that only the central shell region and the two peripheral regions in the direction of each scan fell within this width, which corresponded to 11 pixels or $33''$ in the sky.

The mean H I velocity in the region of the complex that was determined from the emission of "unaccelerated" gas detected on all scans 1–7 outside shells I, II, and III discussed below is $V_{\rm Hel} = -230 \pm 5$ km s^{-1}. This value is in good agreement with the estimate obtained by Lake and Skillman (1989) for this part of the galaxy from low-angular-resolution observations.

Figure 2b shows the radial-velocity variation with distance typical of an expanding shell at least for the two objects denoted by II and III. The characteristic arc-shaped pattern of velocity variation (half of the "velocity ellipse") is seen both on the scans along the pairs of shells I–II and II–III and on the scans that cross each of shells II and III in a perpendicular direction (see Fig. 2b). Evidence of shell-II expansion is seen on scan 1 (370–400 arcsec), scan 2 (180–230 acrsec), and scan 5 (130–170 arcsec). Scan 2 (280–310 arcsec) and scan 6 (140–190 arcsec) exhibit shell-III expansion. In both cases, one side of the expanding shell is clearly seen. The difference between the unaccelerated-gas velocities on the periphery of shell II ($-225 \div -230$ km s^{-1}) and on its approaching side ($-240 \div -242$ km s^{-1}) gives an expansion velocity V(exp) $\sim 12 - 17$ km s^{-1}. For shell III, we find the expansion velocity from the difference between the unaccelerated-gas velocities on the periphery ($-228 \div -230$ km s^{-1}) and on the receding side (-212 km s^{-1}) to be $V(exp) \sim 16 - 18$ km s^{-1}. The neutral shell I exhibits no distinct expansion.

The inferred expansion velocities of the two H I shells in IC 1613 fall within the region of the peak in the velocity distribution of neutral supershells in the LMC (Kim *et al.* 1999).

The only supernova remnant in IC 1613 lies at the outer boundary of the densest H I layer in the galaxy that bounds shell II in the south (see Fig. 2a). Another, fainter neutral shell in which the supernova remnant is located may adjoin the bright shell II in the south. Scan 7 (120–170 arcsec) shows traces of expansion of this fourth neutral shell. The supernova remnant lies at the inner boundary of this shell (~ 120 arcsec). This scenario — a supernova explosion inside a cavity surrounded by a dense shell and a collision of the expanding remnant with the shell wall — was suggested by Lozinskaya *et al.* (1998) to explain the peculiarity of this remnant, which combines the properties of young and old objects and which has high optical and X-ray brightnesses.

The region at the boundary between shells I and II where the chain of early-type giants and supergiants is

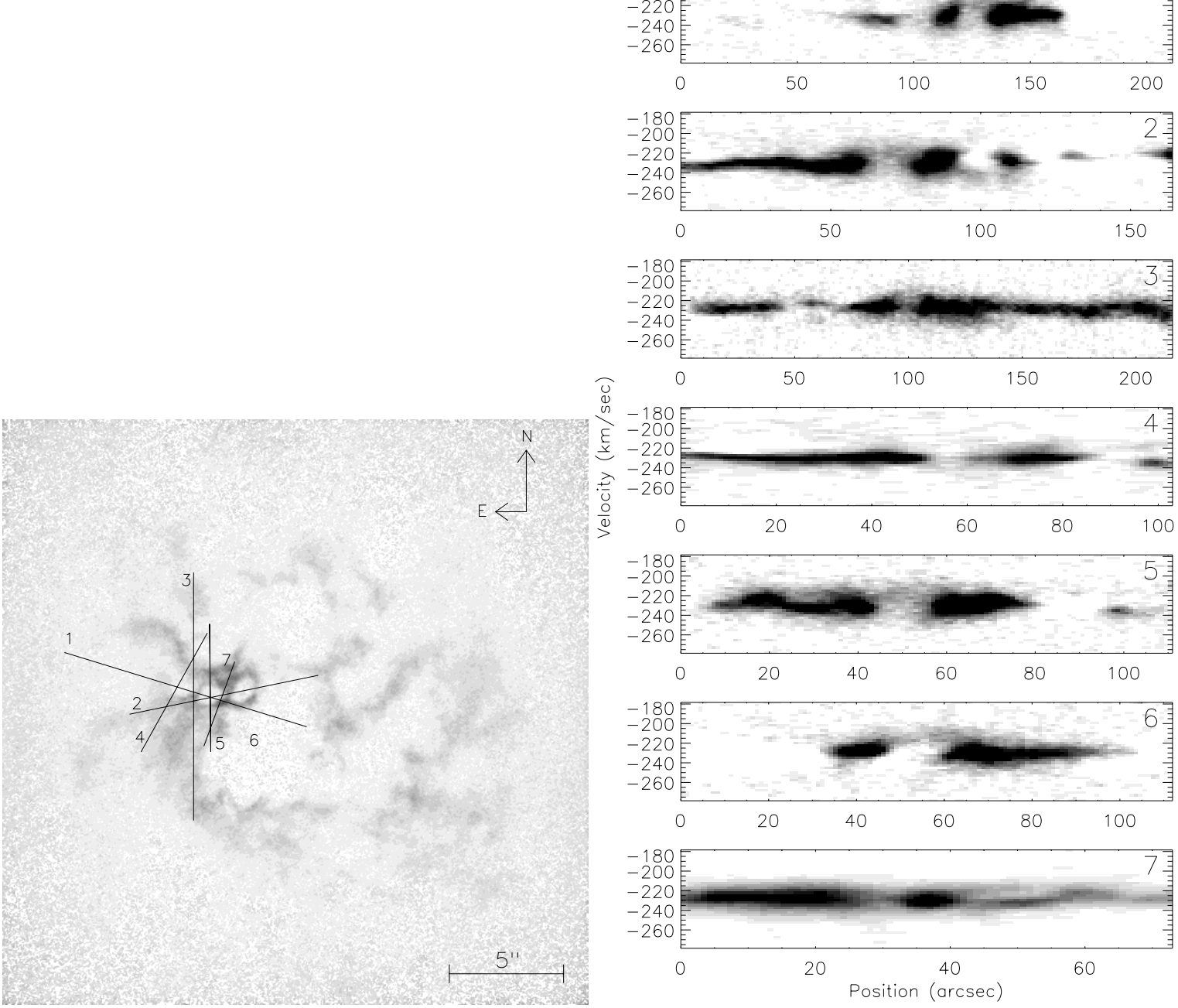

Fig. 2. (a – *left*) The localization of scans 1–7 shown in Fig. 2b on the H I map of the galaxy. The numbers are given at the beginning of each scan. (b – *right*) The position–H I velocity diagrams for scans 1–7 (the velocity is heliocentric).

located exhibits high neutral-gas velocities. A deficit of 21-cm brightness is observed in this region on scan 3 (280–310 arcsec). This deficit stems from the fact that emission from only the thin bar between shells I and II is detected here when scanning. However, this weak emission is observed over a wide velocity range, from $\simeq -250$ to $\simeq -210$ km s^{-1} at 20–30% I(max).

Our expansion velocities and the corresponding kinematic ages of the bright neutral shells in the complex of star formation are given in Table 2.

5. IONIZED-GAS KINEMATICS IN THE COMPLEX

To study in detail the kinematics of the ionized shells using our Hα observations with IFP501, we constructed position–radial velocity diagrams for thirty scans, which cover the entire complex of star formation almost uniformly. For each of the chosen directions, we constructed two or three scans of different widths: from 1 to 40 pixels (from 0.5 to 24″). Figure 3a shows the localization of some of these scans. The width of scans 14 and 17 is 21 pixels

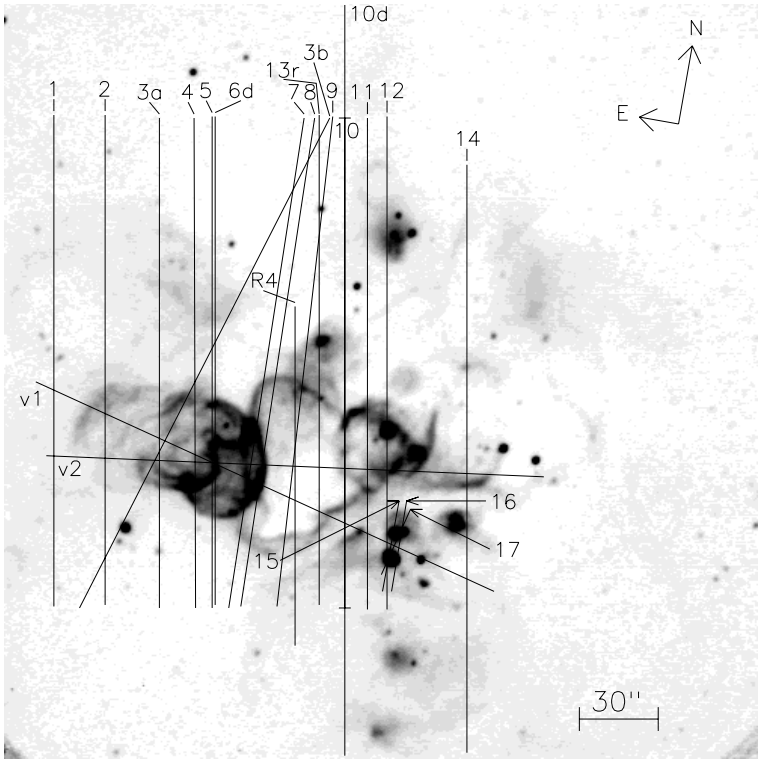

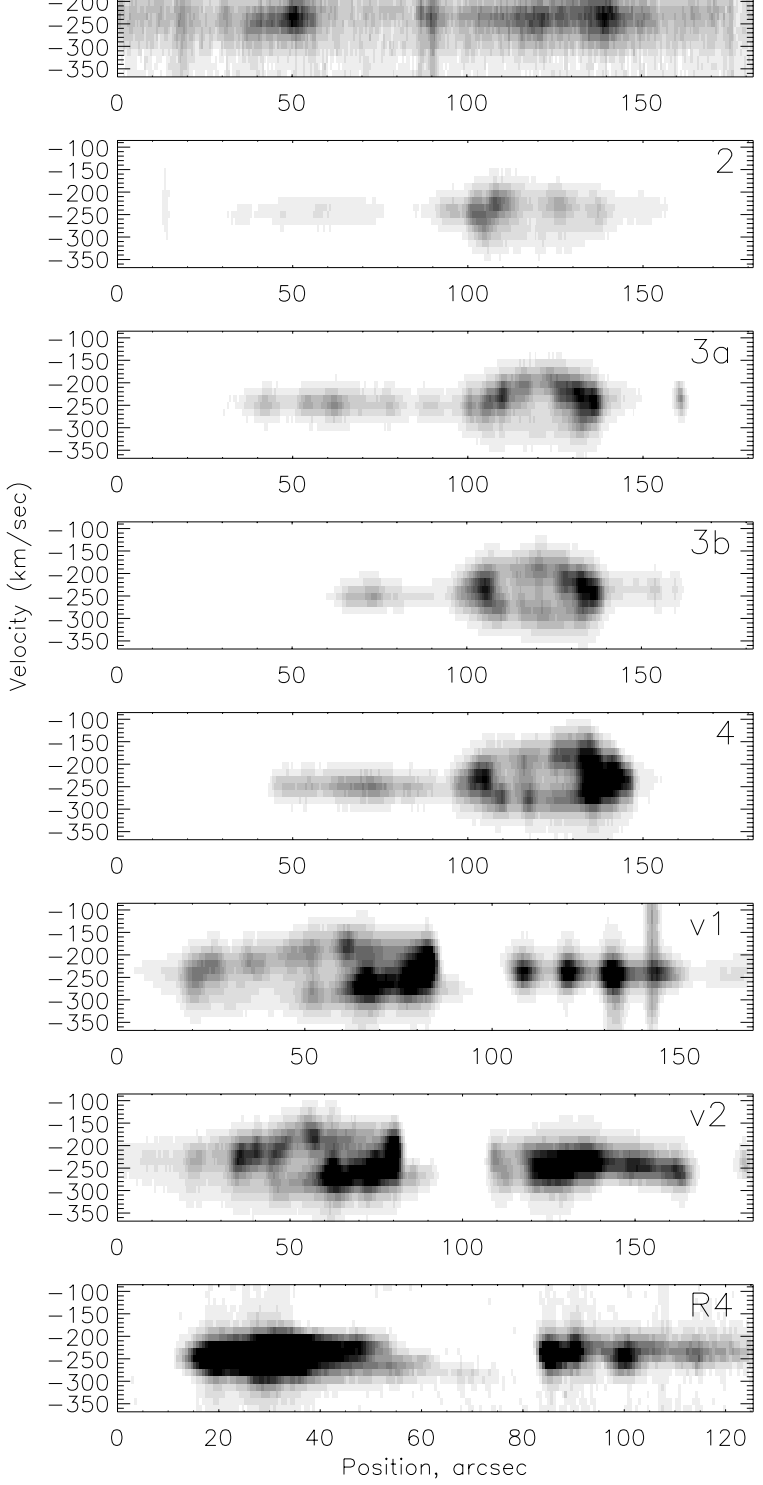

Fig. 3. (a – *left*) The localization of the scans shown in Figs. 3b, 3c, and 3d in the Hα image of the complex. The numbers are given at the beginning of each scan. (b – *right*) The position–H II velocity diagrams for scans nos. 1, 2, 3a, 3b, 4, v1, v2, and R4 (the velocity is heliocentric.)

or 12″; the width of the remaining scans shown in Fig. 3 is 11 pixels or 6″.

The mean velocity of the unshifted feature in the Hα emission in the complex of star formation is $-230 \div -240$ km s^{-1}. We also observe a smooth velocity variation in the complex between -220 km s^{-1} in the southeast and -260 km s^{-1} in the northwest, in agreement with the results of Valdez-Gutierrez *et al.* (2001).

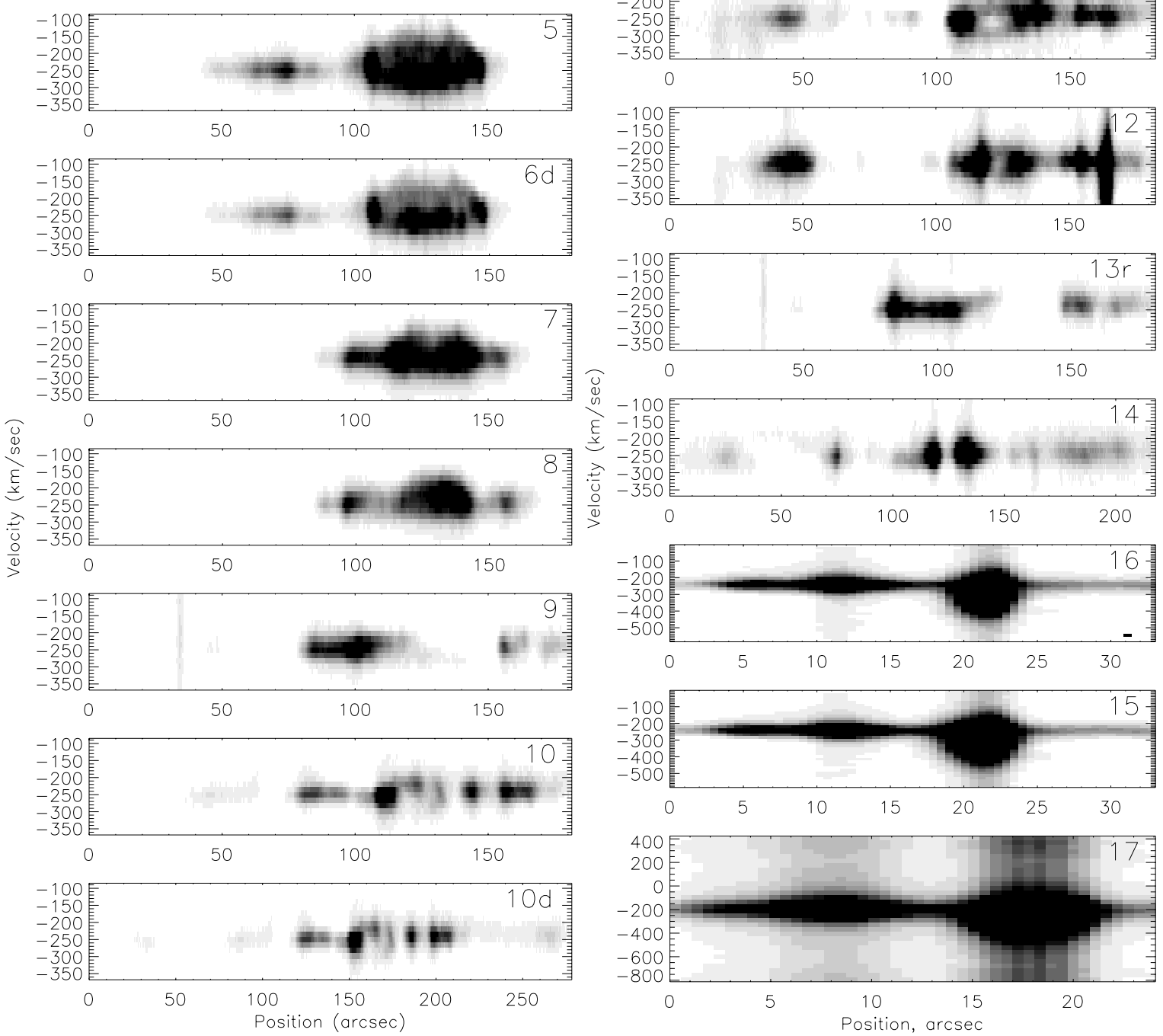

Fig. 3. (c – *left*) Same as Fig. 3b for scans nos. 5, 6d, 7, 8, 9, 10, and 10d. (d – *right*) Same as Fig. 3 for scans nos. 11, 12, 13r, 14, 15, 16, 17.

As was shown in Section 3, the elongated system of brightest ionized shells, including R1, R2, R4, R5, and R6, is associated with the neutral shells I, II, and III.

Two scans (v1 and v2) cross this chain of bright shells in directions that roughly coincide with scans 1 and 2 over the neutral shells I–II and II–III, respectively (see Section 4).

The two scans clearly show Hα line splitting along the entire length of the chain and reveal the characteristic configuration of the velocity ellipse for individual shells and, possibly, for the chain of bright shells as a whole. The typical velocities are about $-290 \div -300$ km s^{-1} for the approaching sides of the elongated system of bright shells and about $-190 \div -200$ km s^{-1} for its receding sides. We successively consider all the ionized shells of this system.

Boundary

Shells R1 and R2 and the region at their boundary where the chain of young stars is located were scanned repeatedly, in different directions, and in bands of different widths. All of the scans passing through the central regions of these shells clearly reveal the characteristic configuration of the velocity ellipse related to their expansion.

The mean velocity of the unperturbed gas at the eastern boundary of shell R1 is -240 km s^{-1}. The local velocity ellipses on scan v2 suggest that the bright western part of shell R1 (45–55 arcsec) expands at a velocity of 50–60 km s^{-1} relative to this unshifted feature: the velocity of the approaching side is -290 km s^{-1}. In shell R2 (55–80 arcsec), the velocities of the bright approaching and faint receding sides are $-280 \div -300$ and -170 km s^{-1}, respectively. On scan v1 that crosses the same region in a different direction, we see a similar arc structure in region R2 and individual clumps in region R1.

Several scans that cross the system of bright shells in the directions perpendicular to v1 and v2 also clearly reveal an expansion of shells R1 and R2. Scans 3a, 3b, and 4 clearly show that shell R1 expands at a velocity of 60–70 km s^{-1} (up to 100 km s^{-1} in its bright southern part). The bright regions on the shell periphery exhibit the unshifted line component at a velocity of $-230 \div -250$ km s^{-1}; the velocities of the two sides of the expanding shell are -180 and -320 km s^{-1} (scan 3). Scan 4 also shows that the bright southern part of shell R1 expands faster than does its northern part: the velocity of the approaching side is the same in the entire shell, being about -300 km s^{-1}; the velocity of the receding side is -150 km s^{-1} in the south and -180 km s^{-1} in the north. Scan 2 that crosses the fainter eastern half of shell R1 also reveals evidence of its expansion. The unshifted features on the shell periphery have a velocity of -240 km s^{-1}, the bright clump in the northern part is observed at a velocity of -215 km s^{-1}, and the faint approaching side has a velocity of -300 km s^{-1}.

Valdez-Gutierrez *et al.* (2001) identified two components in the integrated line profile at velocities of -216 and -274 km s^{-1} in shell R1 and two features at velocities of -244 and -147 km s^{-1} in shell R2. All these values fall within the range determined by the velocity ellipses for these two shells.

The region at the boundary between shells R1 and R2 that, in the 21-cm line, corresponds to the thin bar between the neutral shells I and II, where the chain of early-type stars is located, is represented by scans 5 and 6d. Scan 6d exhibits a bright emission feature in the Hα line at a velocity of about $-270 \div -280$ km s^{-1}, which corresponds to the bright part of shell R1 with the chain of stars, traces of stellar continuum emission, and a weaker emission feature in the region of shell R2 at higher velocities, up to $-130 \div -150$ km s^{-1}. This entire region on scan 6d (105–150 arcsec) widens toward the center, with the dense clumps on the periphery and the gas in an asymmetric gas expansion in shell R2 at a velocity of about 30 km s^{-1} into a denser medium and at a velocity of about 100–110 km s^{-1} into a less dense medium. We associate this effect with shell R2, because the boundary of the expanding region on scan 6d coincides with the boundary of this shell. Scan 5 also exhibits irregular motions of the receding gaseous clumps up to velocities of $-150 \div -160$ km s^{-1}; these are probably related to the local action of the wind from the chain stars. The velocity of the near side of shell R2, which is brighter and more regular, reaches $-280 \div -290$ km s^{-1}. Since the bright clumps on the periphery of the velocity ellipse coincide with the boundaries of shell R2, which is larger than shell R1 here, we believe that the velocity ellipse on scans 6 and 5 also reflects the expansion of shell R2.

Shell R4 and its Possible Collision with Shell R2

R4 is the most extended shell in the chain of bright shells and the only one that completely fits into the surrounding neutral shell. Its central regions are characterized by weak emission. Scans R4, 9, v1, v2, and 13r show a deficit of gas in the central cavity and intense emission on the periphery at a velocity of about -240 km s^{-1}. The weak Hα emission features in the central cavity exhibit a blueshift and a redshift relative to this velocity. Weak diffuse emission is observed at velocities up to -200 km s^{-1} (scan R4, 40–55 arcsec; scan 9, 110–120 arcsec) in the north of the cavity and up to -290 km s^{-1} (scan 4R, 55–70 arcsec; scan 9, 120–130 arcsec) in the south. The shell expansion velocity determined by these features is ~ 45 km s^{-1}.

The monochromatic Hα image shows a characteristic lenticular structure at the boundary between shells R2 and R4. This structure can be a manifestation of the dense gaseous ring formed in the region of head-on collision between these shells and oriented almost edge-on to the observer. The formation of this ring follows from three-dimensional numerical simulations of the collision between two expanding shells [see Chernin *et al.* (1995) and references therein).

In the region that corresponds to the eastern boundary of shell R4 (scan 7, 95–115 arcsec), we see no significant deviations from the mean ionized-gas velocity of -240 km s^{-1} in the complex. The inclined ring in the region of collision with shell R2 is observed as two bright unaccelerated clumps and high-velocity motions between them (scan 7, 120 and 140 arcsec) and as a bright structure with high velocities of the internal motions (scan 8, from 120 to 140 arcsec). The velocities of the faint features between the bright clumps are at a maximum; they reach -140 and -340 km s^{-1} at 7% I(max) on scan 7a and -160 km s^{-1} at 10% I(max) on scan 8.

A characteristic arc structure (110–135 arcsec on scan 10 and 150–175 arcsec on scan 10d) is observed at the boundary between shells R4 and R5. This structure may represent the half of the velocity ellipse that corresponds to the receding side of shell R5. We estimated the expansion velocity to be 40–50 km s^{-1}.

Scan 11 (105–135 arcsec) also shows a symmetric expansion of shell R5 at a velocity of about 35–45 km s^{-1}; the velocities of the two sides of the shell are -220 and -310 km s^{-1}.

A compact group of stars with the only Of star identified in the galaxy (Lozinskaya *et al.* 2002) is located on the periphery of shell R5. Scan 12 shows this star in a region of 118 arcsec; the star is surrounded by a bright compact H II region. Given the IFP501 instrumental profile, the line width in the H II region at $0.5I$(max) is 50 ± 5 km s^{-1}.

Shell R13 and the H II Region no. 55 from the List of Hodge et al. *(1990)*

Shell R13, which adjoins shell R4 in the north, consists of two components: a diffuse shell and the bright compact H II region nos. 55 (Hodge *et al.* 1990). The bright H II region shows a mean velocity of about $-230 \div -240$ km s^{-1} [in agreement with the measurements of Valdez-Gutierrez *et al.* (2001)] and stellar continuum at the center (scan 13r, position 85 arcsec). A group of stars may be located here, because the area of stellar continuum is broader than that in other regions of the same scan. The line width in the bright H II region reaches 57 km s^{-1} at $0.5I$(max).

The diffuse shell R13 also exhibits the mean radial velocity of $-230 \div -240$ km s^{-1} typical of the entire complex. We found no clear evidence of shell-R13 expansion.

Shells R6 and R8

According to our data, the expansion velocity of shell R6 does not exceed 20 km s^{-1}: the velocities of the northern and southern shell boundaries (scan 14, 75 and 120 arcsec, respectively) and the velocity in the central region (about 100 arcsec on the same scan) are about -255 km s^{-1}.

Shell R8 exhibits the characteristic arc-shaped pattern of radial-velocity variation of the far side. The velocity of the bright boundary regions (scan 14, 25 and 75 arcsec) is -255 km s^{-1} and the velocity of the faint far side reaches -190 km s^{-1}, which gives an expansion velocity of about 65 km s^{-1}. We detected no emission from the even fainter near side.

The Bright H II Regions nos. 40,b and 39 (Hodge et al. *1990)*

Valdez-Gutierrez *et al.* (2001) provided the following parameters averaged over the group of objects nos. 40,b and 39: the velocity at the line peak, -239 km s^{-1}, and the velocity dispersion, 10.4 km s^{-1}. We separately scanned the two bright sources no. 40a (scan 16) and no. 40b (scan 15); both also include the emission from the more extended and fainter region no. 39. As follows from Fig. 3f, the velocity at the peak of these three regions is -240 km s^{-1}. The H II region no. 39 is characterized by a narrow Hα line with no wings with the FWHM determined by the IFP501 instrumental profile along the entire length. At the same time, both bright compact H II regions nos. 40a and 40b (scans 16 and 15, respectively) exhibit weak emission at 10% I(max) in the velocity range from -310 to -175 km s^{-1}.

Shell	Size, pc	V_{exp}, km s^{-1}	V_{exp}(V–G), km s^{-1}	Age, Myr
R1	188×138	60–75	29	0.7 (81/67)
R2	145×88	50–60	49	0.6 (58/55)
R3	258×209		30	1.9 (V–G)
R4	234×138	40–45	32	2.2 (93/42)
R5	113×113	30–50	38	0.8 (56/40)
R6	226×184	≤ 20	25	2.0 (V–G)
R8	217×154	$\simeq 65$	26	1.7 (185/65)

The Supernova Remnant

The bright nebula S8 (Sandage 1971), the supernova remnant, shows emission over the entire velocity range from 0 to -600 km s^{-1} determined by the IFP501 free spectral range (scans 15 and 16, 19–23 arcsec). The remnant emission is observed with IFP235 at least in the velocity range from $+200$ to -600 km s^{-1} (scan 17). An interfering emission emerges at higher velocities, $+400$ and -800 km s^{-1}. This emission is probably attributable to an improper allowance for the night-sky 6554 Å line.

This result is in complete agreement with previous observations of Lozinskaya *et al.* (1998) and Rosado *et al.* (2001).

All of the ionized shells in the complex of star formation for which we managed to reliably detect their expansion based on the velocity ellipse are collected in Table 3. For comparison, the fourth column of the table gives the expansion velocities of the same shells determined by Valdez-Gutierrez *et al.* (2001) from line-profile splitting. Since the shell sizes were measured from our deep images, they slightly differ from those of Valdez-Gutierrez *et al.* (2001). It should be noted that, given the irregular shape of most shells, the representation of the observed shells by regular ellipses is arbitrary and subjective in nature.

In estimating the kinematic ages of the shells from their radii and expansion velocities, we used the classical theory of wind blown bubble ($t = 0.6\ R/V$). In addition to the age, the mean radius and expansion velocity used for its estimation are given in parentheses (in the form R/V) in the last column of the table. The ages of

6. DISCUSSION

The radial-velocity variations with distance from the center of the ionized shells (velocity ellipses) found here are generally in agreement with the observations of Meaburn *et al.* (1988) and Valdez-Gutierrez *et al.* (2001) but they give a clearer picture of expansion. In the latter paper, the conclusions regarding expansion were drawn from integrated line profile splitting in the shells. Since bright peripheral regions or individual bright clumps can give a significant contribution when averaging over the shell or over its separate fields, the expansion velocity determined in this way can be underestimated. The large brightness difference between the approaching and receding sides of the shells can also cause the expansion velocity inferred from line splitting to be underestimated. The constructed velocity ellipses allow these difficulties to be circumvented. The expansion velocity can be determined from the velocity ellipse by taking into account the geometrical projection even if only one shell side is observed, as in the case of R8. Indeed, as we see from Table 3, our estimates of the expansion velocity in most shells gave higher values than those in Valdez-Gutierrez *et al.* (2001).

In several shells, we detected a distinct asymmetry in their expansion: the approaching and receding sides have different velocities.

On scans v1 and v2 crossing the entire chain of the brightest ionized shells, we clearly see that all of them generally have similar velocities but an irregular, clumpy brightness distribution. This irregular brightness distribution may have served as the basis for the conclusion of Valdez-Gutierrez *et al.* (2001) that shells R1 and R2 are at different distances, because they are observed at different radial velocities. These scans show that individual bright clumps on the two sides of these shells actually have different velocities but they all fall within our velocity ellipses. According to our measurements, the approaching and receding sides of the two shells have similar velocities: $-290 \div -320$ and $-170 \div -190$ km s^{-1}, as inferred from different scans in R1; $-280 \div -300$ and -170 km s^{-1} in R2. The far side is brighter in R1 and the near side is brighter in R2. We also noted that the southern part of shell R1 recedes faster ($V = -150$ km s^{-1}) than does its northern part ($V = -180$ km s^{-1}).

Taking into account the structure of R1 and R2 in different velocity ranges, we do not rule out the possibility that these shells generally constitute a single dumbbell-like structure formed on both sides of a dense neutral-gas layer. However, this assumption requires additional observational confirmation.

Valdez-Gutierrez *et al.*. (2001) showed that the energy of the stellar wind from nearby associations was enough for most of the ionized shells to be formed. The rapidly expanding shells R1 and R2 constitute an exception. We further increased the expansion velocity of these two ob-

most intense sources of the stellar wind at their boundary — early-type supergiants and giants (Lozinskaya *et al.* 2002), which removes the problem of the mechanical energy sources.

Recall also that the two mentioned shells R1 and R2 exhibit an intense emission in the [S II] 6717/6731 Å lines (see Valdez-Gutierrez *et al.* 2001; Lozinskaya *et al.* 2002), typical of the radiation of the shock waves generated by a supernova explosion.

The neutral shells produced by the combined effect of the wind and supernovae in associations are being widely searched for in nearby galaxies (see, e.g., the review article by Brinks 1994; Kim *et al.* 1999; Oey *et al.* 2002; and references therein). In most cases, the 21-cm observations either do not reveal any distinct neutral-gas shell structure around associations at all or do not allow the neutral-gas structures to be unambiguously associated with H II shells. The studies of neutral gas in the vicinity of the three well-known ionized supershells in the LMC carried out by Oey *et al.* (2002) serve as a clear example.

The complex of star formation in IC 1613 constitutes a lucky exception. We do not know any other examples of such a distinct interaction between multiple ionized and neutral shells that is observed in the complex under discussion.

Here, we have studied the kinematics of the identified neutral shells I, II, and III for the first time. We have also detected expansion and measured the expansion velocity for the first time.

As was mentioned in Section 3, the derived radii and expansion velocities of the H I shells in IC 1613 fall within the region of the peak in the distribution of neutral shells in the LMC and SMC in size and expansion velocity. The age of the H I shells in the complex of star formation in IC 1613 (5.3–5.5 Myr) is also in complete agreement with the peaks in the age distributions of H I supershells in the LMC (4.9 Myr; Kim *et al.* 1999) and in the SMC (5.4 Myr; Staveley-Smith *et al.* (1997).

We estimated the kinematic ages of the neutral shells II and III in Table 2 from their mean radii and expansion velocities by using the classical theory of a constant stellar wind in a homogeneous medium. This assumes that the mechanical luminosity of the wind from the association stars responsible for the shell formation does not vary with time and that all stars were formed simultaneously. Of course, both assumptions are not valid, although they are universally accepted. Allowance for sequential star formation and for variations in the mass loss rate during the evolution of a rich association as well as for the cloudy structure of the interstellar medium can change the age estimate by a factor of 1.5 to 3 (see, e.g., Shull and Saken 1995; Oey *et al.* 1996; Silich *et al.* 1996; Silich and Franco 1999; and references therein). Nevertheless, we may conclude that the derived ages of shells II (5.6 Myr) and III (5.3 Myr) agree with the ages of the stellar associations in the complex of star formation. Shell I, whose

The three-color photometry of stars in IC 1613 performed by Hodge *et al.* (1991) gave a minimum age of the stars in their field no. 1, where the neutral shells that we identified are located, equal to 5 Myr. This field includes associations nos. 10, 12, 13, 14, 15, and 17 from the list by Hodge (1978), whose mean and minimum ages were estimated by Hodge *et al.* (1991) to be 17 and 3 Myr, respectively. Recent estimates by Georgiev *et al.* (1999) yielded similar results: the age of the youngest nearby associations nos. 10 and 14 is about 5 Myr and the age of the oldest associations (nos. 12, 19, and 19) reaches 20 Myr.

The mechanical wind luminosity that is required for the neutral shells observed in the complex to be formed and that is determined by using the classical model (with all of the reservations made above) is 5×10^{38}, 5×10^{37}, and 5×10^{36} erg s^{-1} in a medium with an initial density of 10, 1, and 0.1 cm^{-3}, respectively. These values seem reasonable enough for the stars found in the region — the sources of a strong stellar wind (see Valdez-Gutierrez *et al.* 2001; Lozinskaya *et al.* 2002). It should be emphasized, however, that the spectra of bright stars in the region are required to adequately discuss the sources of mechanical energy. Lozinskaya *et al.* (2002) obtained the spectra of stars only in three small fields of the star-forming complex and detected stars with strong winds, blue supergiants and Of star, in two of them.

Despite the "suitable" age and input of mechanical energy, we do not consider it possible to unequivocally associate the formation of neutral shells with the action of the stellar wind from the OB associations identified by Georgiev *et al.* (1999) for the following reasons.

First, most of the H I supershells identified in the LMC, the SMC, and other Local-Group galaxies are several-fold younger than the corresponding OB associations (see, e.g., Kim *et al.* 1999; Staveley-Smith *et al.* 1997, and references therein). Therefore, it may well be that the H I shells that we detected in IC 1613 were also formed by an older population than the young groups of stars shown in Fig. 1c.

As follows from Table 3 and from similar estimates by Valdez-Gutierrez *et al.* (2001), the ages of most of the ionized shells in the complex lie within the range from 0.6 to 2.2 Myr. These ages are much younger than the ages of the OB associations that could be responsible for their formation. Such a situation is observed in most galactic and extragalactic ionized shells and supershells. In general, to explain this mismatch, either noncoeval star formation is assumed or the shells are assumed to be formed only by stars at a late evolutionary stage — WR, Of, and BSG with a short-duration, but intense wind. The situation in the complex under consideration is more complicated, because the bright ionized shells are localized inside or at the boundary of the older neutral shells and their evolution differs significantly from the standard theory.

In addition, a number of observed facts actually suggest noncoeval star formation in the complex.

tions in the region are localized not at the center but in the dense peripheral parts of the H I shells [the only association no. 7 from the list by Georgiev *et al.* (1999) is partly located inside shell III). In general, this picture may provide evidence for the formation of these associations in dense H I shells. We emphasize that the new association boundaries delineated by Georgiev *et al.* (1999) split the associations of Hodge (1978) into smaller groups, which are believed to be the young nuclei of the corresponding associations. The scenario for triggered stars formation in expanding shells was considered by many authors [see, e.g., Elmegreen *et al.* (2002) and references therein].

Comparison of the ages and mutual localizations of the ionized and neutral structures in the complex also suggests noncoeval star formation. All the ionized shells are several-fold younger than the neutral shells. As was pointed out in Section 3, most of the bright ionized shells are located in the dense peripheral parts of the H I shells. The only exception is shell R4, which completely fits into the neutral shell II from the inside. According to our measurements, this ionized shell is oldest and all the young nuclei of the OB associations are located in its boundary regions (see Fig. 1c).

However, these arguments for sequential or triggered star formation, which refer to the neutral shells of the complex studied in detail here, are speculative, because the age difference between the H I and H II shells is small.

The multishell complex itself, which represents the only region of violent ongoing star formation in IC 1613, may have been produced by the collision of two older and more massive giant neutral supershells (Lozinskaya 2002a, 2000b). Indeed, in addition to the three bright and relatively small H I shells considered here, a giant H I ring south of the star-forming complex and a giant arc structure in the north, which probably also represents part of the neutral supershell, can be identified in Fig. 2a. The characteristic size of the two structures is $\sim 1{-}1.5$ kpc. The complex of ongoing star formation lies at their common boundary, where the collision of these two giant supershells could trigger violent star formation. We are planning to consider this scenario in detail.

7. CONCLUSIONS

We studied in detail the structure and kinematics of the neutral and ionized gas components in the only known complex of star formation in the irregular dwarf galaxy IC 1613.

To study the kinematics of the ionized shells, we carried out Hα observations with a scanning Fabry–Perot interferometer attached to the 6-m SAO telescope. The monochromatic Hα image of the multishell complex obtained from our interferometric observations reveals new faint filamentary structures in several regions of the complex.

We constructed position–radial velocity diagrams, which cover the entire complex of star formation almost

tance from the center, the velocity ellipse, was used to refine (increase) the expansion velocities of most ionized shells in the complex estimated by Valdez-Gutierrez *et al.* (2001). The expansion in several shells was found to be asymmetric: the approaching and receding sides of the shells have different velocities.

Based on our VLA 21-cm observations, we have studied the neutral-gas kinematics in the complex of star formation for the first time. The mean H I velocity in the complex is $V_{\rm Hel} = -230 \pm 5$ km s^{-1}, in good agreement with the estimate obtained by Lake and Skillman (1989) for this part of the galaxy from low-angular-resolution observations.

We identified three extended (300–350 pc) neutral shells with which the brightest ionized shells in the complex of star formation are associated. The two H I shells were found to expand at a velocity of 15–18 km s^{-1}.

The sizes, expansion velocities, and kinematic ages of the neutral shells in the complex fall within the regions of the peaks in the corresponding distributions for giant shells in the LMC and SMC.

We identified an incomplete H I shell with the only known supernova remnant in the galaxy located at its inner boundary. This confirms the scenario for a supernova explosion inside a cavity surrounded by a dense shell and a collision of the remnant with the shell wall suggested by Lozinskaya *et al.* (1998) to explain the peculiarity of this remnant, which combines the properties of young and old objects.

We found evidence of the physical interaction between the H I and H II shells in the region of the chain of stars, early-type giants and supergiants, detected by Lozinskaya *et al.* (2002). The region at the boundary of the two shells where the stellar chain is located was shown to be the dynamically most active part of the star-forming complex. The highest H II and H I velocities are observed here.

The relative positions and ages of the H I and H II shells and OB associations in the complex suggest sequential or triggered star formation in the expanding neutral shells.

In addition to the three brightest and most prominent H I shells, we found supergiant arches and ring structures in the galaxy whose sizes are comparable to the gaseous-disk thickness. These may be assumed to be the traces of preceding starbursts in IC 1613.

ACKNOWLEDGMENTS

This study was supported by the Russian Foundation for Basic Research (project nos. 01-02-16118 and 02-02-06048mas), the Federal Central Research Program (contract 40.022.1.1.1102), and CONACYT (Mexico, project 36132-). The observational data were obtained with the 6-m SAO telescope financed by the Ministry of Science of Russia (registration number 01-43). We are grateful to the 6-m Telescope Committee for allocating observational time. The National Radio AStronomy Observatory (USA) and is operated by the Association of Universities Inc. under a contract with the NSF. We wish to thank S.A. Silich who read the manuscript for helpful remarks.

References

V. L. Afanas'ev, T. A. Lozinskaya, A. V. Moiseev, and E. Blanton, Astron. Lett. **26**, 153 (2000) (astro-ph/0011385)
E. Brinks, in *Violent Star Formation from 30 Doradus to QSOs,* Ed. by G. Tenorio-Tagle (Cambridge Univ. Press, Cambridge, 1994), p. 145.
A. D. Chernin, Yu. N. Efremov, and P. A. Voinovich, Mon. Not. R. Astron. Soc. **275**, 313 (1995).
A. D. Chernin and T. A. Lozinskaya, Astron. Astrophys. Trans., **21**, 231 (2002)
A. Dolphin, A. Saha, E. D. Skillman, *et al.*, Astrophys. J. **550**, 554 (2001).
B. G. Elmegreen, J. Palous, and S. Ehlerova, Mon. Not. R. Astron. Soc. **334**, 693 (2002).
W. Freedman, Astrophys. J. **326**, 691 (1988a).
W. Freedman, Astron. J. **96**, 1248 (1988b).
L. Georgiev, J. Borissova, M. Rosado, *et al.*, Astron. Astrophys., Suppl. Ser. **134**, 21 (1999).
P. W. Hodge, Astrophys. J., Suppl. Ser. **37**, 145 (1978).
P. Hodge, M. G. Lee, and M. Gurwell, Publ. Astron. Soc. Pac. **102**, 1245 (1990).
P. W. Hodge, T. R. Smith, P. B. Eskridge, *et al.*, Astrophys. J. **369**, 372 (1991).
D. A. Hunter, W. N. Hawley, and J. S. Gallagher, Astron. J. **106**, 1797 (1993).
S. Kim, M. A. Dopita, L. Staveley-Smith, and M. S. Bessell, Astron. J. **118**, 2797 (1999).
G. Lake and E. D. Skillman, Astron. J. **98**, 1274 (1989).
J. Lequeux, N. Meysonnier, and M. Azzopardi, Astron. Astrophys., Suppl. Ser. **67**, 169 (1987).
T. A. Lozinskaya, Astron. Astrophys. Trans., **21**, 223 (2002a)
T. A. Lozinskaya, Publ. of ASP Conference ser., *"Seeng Through the Dust: The Detection of HI and the Exploration of the ISM of Galaxies", Penticton, Canada* Ed. by R. Taylor, T. Landecker, and T. Willis, **276**, 374 (2002b)
T. A. Lozinskaya, O. K. Silchenko, D. J. Helfand, and M. W. Goss, Astron. J. **116**, 2328 (1998).
T. A. Lozinskaya, A. V. Moiseev, V. L. Afanas'ev, *et al*, Astron. Rep. **45**, 417 (2001) (astro-ph/0103312)
T. A. Lozinskaya, V. P. Arkhipova, A. V. Moiseev, and V. L. Afanasiev, Astron. Rep. **46**, 16 (2002) (astro-ph/0206397)
I. Meaburn, Mon. Not. R. Astron. Soc. **192**, 365 (1980).
J. Meaburn, C. A. Clayton, and M. J. Whitehead, Mon. Not. R. Astron. Soc. **235**, 479 (1988).
A. V. Moiseev, Bull. of SAO, **54**, (2002) (astro-ph/0211104)
M. S. Oey, Astrophys. J. **467**, 666 (1996).
M. S. Oey, B. Groves, L. Staveley-Smith, and R. C. Smith, Astron. J. **123**, 255 (2002).
J. S. Price, S. F. Mason, and C. A. Gullixson, Astron. J. **100**, 420 (1990).
M. Rosado, M. Valdez-Guterrez, L. Goergiev, *et al.*, Astron. J. (in press) (2001).
A. Sandage, Astrophys. J. **166**, 13 (1971).
J. M. Shull and J. M. Saken, Astrophys. J. **444**, 663 (1995).
S. A. Silich, J. Franco, J. Palous, and G. Tenorio-Tagle, Astrophys. J. **468**, 722 (1996).
S. A. Silich and J. Franco, Astrophys. J. **522**, 863 (1999).

M. Valdez-Gutierrez, M. Rosado, L. Georgiev, *et al.*, Astron. Astrophys. **366**, 35 (2001).

Translated by V. Astakhov